Feed-forward and visual feed-back control of head roll orientation in wasps (*Polistes humilis*, Vespidae, Hymenoptera).

Stéphane Viollet[(1)] and Jochen Zeil [(2)]

[(1)] Aix-Marseille Université, CNRS, ISM UMR 7287, 13288, Marseille Cedex 09, France.
email: stephane.viollet@univ-amu.fr

[(2)]ARC Centre of Excellence in Vision Science, Research School of Biology, The Australian National University, Biology Place, Bld. 46, Canberra, ACT 0200, Australia.
email: jochen.zeil@anu.edu.au

Address for correspondence: stephane.viollet@univ-amu.fr

Keywords: *Polistes* wasps, Head roll control, Vision, Efference copy, feed-forward control, Modelling, Visuo-motor feedback loop, Gaze control.

Running title: Modelling visual head stabilization in wasps.

Abstract

Flying insects keep their visual system horizontally aligned suggesting that gaze stabilization is a crucial first step in flight control. Unlike flies, hymenopteran insects, such as bees and wasps do not have halteres that provide fast, feed-forward angular rate information to stabilize head orientation in the presence of body rotations. We tested whether hymenopteran insects use inertial (mechano-sensory) information to control head orientation from other sources, such as the wings, by applying periodic roll perturbations to male *Polistes humilis* wasps flying in tether under different visual conditions indoors and in natural outdoor conditions. We oscillated the insects' thorax with frequency modulated sinusoids (chirps) with frequencies increasing from 0.2Hz to 2Hz at a maximal amplitude of 50° peak-to-peak and maximal angular velocity of ±245°/s. We found that head roll stabilization is best outdoors, but completely absent in uniform visual conditions and in darkness. Step responses confirm that compensatory head roll movements are purely visually driven. Modelling step responses indicates that head roll stabilization is achieved by merging information on head angular velocity presumably provided by motion-sensitive with information on head orientation, presumably provided by light level integration across the compound eyes and/or ocelli (dorsal light response). Body roll in free flight reaches amplitudes of ±40° and angular velocities greater than 1000°/s, while head orientation remains horizontal for most of the time to within ±10°. In free flight, we did not find a delay between spontaneous body roll and compensatory head movements and suggest that this is evidence for the contribution of a feed-forward control to head stabilization.

Introduction

Hymenopteran insects, such as honeybees and solitary wasps stabilize their head around roll and pitch axes during flight (Zeil *et al*., 2008; Boeddeker and Hemmi, 2009; Boeddeker *et al*., 2010). Such compensatory head movements have been thoroughly studied in flies, where a significant contribution to head stabilization comes from non-visual, mechano-sensory input from modified wings, called halteres (Hengstenberg, 1993; Nalbach, 1993, 1994, Nalbach and Hengstenberg, 1994, Dickinson, 1999; Sherman and Dickinson, 2003, Fox and Daniel, 2008; Huston and Krapp, 2009, Frye, 2009). Here we ask whether compensatory head movements in hymenopteran insects, which lack the fast, feed-forward, mechano-sensory input from Coriolis-force sensing modified wings, are driven in addition to visual (Boeddeker and Hemmi, 2009) also by mechano-sensory input that may be originating from mechanoreceptors on the wings, as suggested by Pix *et al*. (1993) or at the base of the antennae, as it has been demonstrated in moths (Sane *et al*., 2007).

We used *Polistes* wasp males in this study, rather than honeybees, because (1) they readily fly when tethered and (2) continue doing so in the dark. We oscillated the tethered wasps around the roll axis in different visual conditions: within an opaque, horizontal cylinder in complete darkness, with an homogeneously illuminated, featureless white wall, with a horizontal pattern of regular black and white stripes, with an artificial horizon, in full view of a cluttered and well-lit indoor environment and of a natural visual environment outdoors. We found no evidence for mechano-sensory input to the system that stabilizes the head around the roll axis in these wasps. To explain visual control of head roll, we provide a control scheme for purely visually-mediated head stabilization based on two nested visual feedback loops involving the measurement of head angular rate and its orientation. We also analysed head roll control in free flight and suggest that its delay-less compensation for body roll is evidence for an efference copy of the body control input signal in spontaneous roll manoeuvres.

Material and methods

General procedure

Male wasps *(Polistes humilis)* were captured at their nest, kept in foam-stopper vials and provided with sugar solution on cotton tips. Before preparing a wasp for an experiment we always checked whether the wasp could fly by releasing and recapturing it indoors. Wasps were held in a foam clamp and a small piece of cardboard was waxed to the thorax. The wasps were then fixed coaxially to the shaft of a servomotor via a flexible wire and a tiny clip that held the small piece of cardboard (Figure 1). The data we present are all from wasps that flew in this tethered state.

Experimental setup

A servomotor (Faulhaber 0620C006, reduction gear ratio of 1024) was mounted on an optical bench so that its centre shaft faced a digital camera (PointGrey Firefly MV) (Figure 1A). The motor and the camera were controlled via a data acquisition board (National Instrument USB 6128) and a Firewire bus. The shaft of the servomotor, the insect head and the optical axis of the camera were carefully aligned by means of two perpendicular translation stages mounted on the motor shaft, by adjusting the height and orientation of the camera above the optical bench and by adjusting the flexible wire that held the insect. We assured proper alignment by minimizing the translational movements of the head during rotations. The motor with the attached insect was then pushed inside an opaque cylinder (diameter 8.5 cm, length 10 cm) that was mounted on a fibre optics ring-light (Schott) connected to a cold light source (Schott KL 1500). The wasp was in addition illuminated by three pairs of infrared LEDs (OPE5685, wavelength 850nm), arranged coaxially around the camera lens to record head movements in darkness. A gentle air stream was generated by a small fan beside the camera pushing air past the camera lens towards the flying insect. The inside of the cylinder carried three different black and white patterns (Fig. 1B): equally spaced horizontal stripes of 1.25 cm width (spatial frequency of 0.03 cycles/°), a 180^{o} black, 180^{o} white pattern forming an artificial horizon and a white piece of paper. Our patterns extended 200^{o} in both azimuth and elevation at the head of the wasps and thus covered 56% of the panoramic visual field with ±40^{o} in the frontal and in the

caudal visual field remaining not stimulated by the patterns inside the cylinder. Experiments inside the cylinder were performed in a completely dark room. In addition, we recorded compensatory head movements without the cylinder so that wasps viewed the well-lit indoor environment of the laboratory and by taking the whole set-up outdoors, where the wasps were exposed to sunny midday light intensities in a natural scene including trees and the artificial structures of a courtyard, surrounded by large buildings. We measured light levels in these different conditions with an ILT 1700 radiometer (International Light Technologies) equipped with a Factor 1 Sensor W12826 to be: dark ($0.04x10^{-9}$ W/cm^2); uniform ($1.95x10^{-3}$ W/cm^2); horizon ($2.38x10^{-3}$ W/cm^2); stripes: $2.13x10^{-3}$ W/cm^2); room light ($2.85x10^{-4}$ W/cm^2); outdoors ($3.3x10^{-2}$ W/cm^2). Light was measured with a horizontally oriented cosine sensor placed at the position of the insect facing into the drum or outdoors at the location of the wasp head facing forwards.

Recording sessions

We recorded head movements around the roll axis by placing a wasp about 10cm in front of the camera (Fig. 1C). We measured the performance of head roll compensation by applying a sine-wave oscillation with linearly increasing frequency from 0.2Hz to 2Hz, called a chirp signal with maximal amplitude of 50° peak-to-peak and a maximal angular velocity of ± 245°/s (Fig. 1D). The amplitude of the oscillation decreased with increasing frequency (see Fig. 2) due to the dynamics of the brushless servomotor. We also employed a fast ramp signal with the same maximal angular velocity to check for the presence of position error signals monitoring the orientation of the head. Both chirp and ramp signals were applied to the servomotor that was rigidly coupled to the thorax of the wasp. Images were captured at 50 frames/s for the chirp signal and at 120 frames/s for the ramp signal, with a resolution of 640 x 480 pixels. The synchronization between servomotor and image acquisition was achieved with a custom-written Labview-based program (National Instruments Corp.) running on a PC. In darkness, the image acquisition was synchronized with flashes produced by the infrared ring-light. Video sequences were stored frame by frame as uncompressed 8-bit tiff images for off-line processing.

Data analysis

The head orientation (θ_{head}) and body orientation (θ_{body}) of wasps were manually digitized with a custom-written Matlab-based (Mathworks, Nattick, USA) program (Jan Hemmi and Robert Parker, The Australian National University) by recording frame-by-frame the x/y positions of two markers at the lateral-most part of the head and two markers on the piece of cardboard that was attached to the thorax of the wasp (see Fig. 1C). By definition, we have the following relationship between θ_{head} and θ_{body}:

$$\theta_{body} + \theta_{headbody} = \theta_{head} \quad (1)$$

with $\theta_{headbody}$ being the angular position of the head with respect to the body.

For perfect compensation of a rotational movement of the body (in our case around the roll axis), the angular orientation $\theta_{headbody}$ must be equal and opposite to θ_{body}. For the ideal case of $\theta_{head} = 0$, equation (1), becomes $\theta_{headbody}(t) = -\theta_{body}(t)$. This means that the transfer function H(s) between θ_{body} and $\theta_{headbody}$ must be equal to -1 in the case of perfect compensation. To summarize, we have:

$$H(s) = \frac{\theta_{headbody}(s)}{\theta_{body}(s)} = -1 \quad (2)$$

with *s* being the Laplace variable.

By definition, equation (2) means that in the case of perfect compensation, the module of H(s), denoted $|H(j\omega)| = 1$ (i.e., 0dB) and the phase denoted $Arg(H(j\omega)) = -180°$, with ω the frequency in rad s^{-1}.

To determine the Bode diagram, we estimated the gain ($|H(j\omega)|$) and phase ($Arg(H(j\omega))$) of the transfer function H(s) as follows:

$$H(s) = \frac{\theta_{headbody}}{\theta_{body}} \quad (3)$$

Therefore, from (3) the gain and phase of H(s) were computed as follows:

149 $$\left|H(j\omega)\right|_{dB} = \frac{\left|\theta_{head} - \theta_{body}\right|}{\left|\theta_{body}\right|} = \frac{\left|\theta_{headbody}\right|}{\left|\theta_{body}\right|} \text{ and } Arg(H(j\omega)) = Arg\left(\frac{\theta_{headbody}}{\theta_{body}}\right)$$

150 The frequency response of H(s) was then estimated by applying spectral analysis on the time
151 series of θ_{body}, $\theta_{headbody}$ and θ_{head} (using the Matlab System Identification Toolbox 'spa'
152 function, see Ljung, 1999 for further details). As discussed by Xia (1997), the use of a chirp
153 signal combined with a spectral analysis method allows one to use an efficient noise
154 reduction technique based on the Fourier transform for the estimation of the transfer
155 function of a linear system. Due to its better noise immunity, we therefore preferred
156 spectral analysis over the classical method based on the Fourier transform (see Schwyn *et*
157 *al.,* 2011). The transfer function of a dynamical system can be directly estimated from the
158 ratio of the Fourier transform of the output signal (here $\theta_{headbody}$) to the Fourier transform of
159 the input signal (here θ_{body}). For most of the time, irregularities and noise make this method
160 (which has been called frequency analysis) difficult to use for the determination of the
161 phase directly (see Ljung, 1996). We, therefore, preferred to use spectral analysis because it
162 is less sensitive to noise. Spectral analysis allows one to estimate directly the transfer
163 function from input and output signals by estimating the cross-spectrum between two
164 signals (here θ_{body} and $\theta_{headbody}$) and the auto-spectrum of the input signal (here θ_{body}) (see
165 Ljung, 1996, 1999). The cross-spectrum is defined by the Fourier transform of the cross-
166 covariance function, whereas the auto-spectrum is the Fourier transform of the cross-
167 spectrum with itself. The quality of the estimation depends on the Fourier transform
168 method. A classical windowing method based on the Hamming window is the most common
169 window used in spectral analysis. The choice of the window size is a pure trade-off between
170 frequency resolution and the variance of the estimation.

171 The mean gain error is the mean of the error between the mean value of the gain $|H(j\omega)|$ of
172 each wasp and 0dB as follows:

173 $Mean\_Error_{gain} = mean(0_{dB} - mean(|H(j\omega)|)$

174 The mean phase error is the mean of the error between the mean value of the phase
175 $Arg(H(j\omega))$ of each wasp and -180° as follows:

$Mean\_Error_{phase} = mean(180° – mean(Arg(H(j\omega)))$

When there was no compensation of the head orientation induced by roll movements of the thorax, it was not possible to compute the Bode diagram. In such cases we computed the cross-correlation between $\theta_{headbody}$ and θ_{body} and the autocorrelation function of θ_{body}.

Free flight recordings

Male *Polistes* wasps were filmed from behind with a horizontally levelled Casio Exilim EX-F1 camera at 300fps as they were regularly patrolling while often facing the branches of a *Magnolia* tree in Canberra, Australia in the autumn of 2012 (see Supplementary Material Movies). The camera was about 2 m away from the scene and viewed a recording area of 23.7x17.8 cm (6.8x5.1^{o}) at an image size of 512x384 pixels. Perspective distortions were thus minimal. However, there are two remaining sources of errors in determining head and body roll orientations. One are errors in determining x/y coordinates from films (see below) and the other are errors introduced by the fact that although the wasps' flight paths were clearly perpendicular to the camera viewing direction, the orientation of the wasps' longitudinal body axis was not always parallel to the optical axis of the camera. This introduces errors into the determination of body roll orientation, because it confuses body yaw movements with roll movements. In order to identify the parts of sequences in which the camera viewed animals from straight behind, we estimated their yaw orientation by the horizontal distance between the head and the tip of the abdomen (Fig. 1E), after having determined the average length of the longitudinal body axis of wasps to be 1.48 ± 0.08 cm (n = 16) from instances where wasps were clearly seen side-on (see Fig. S1). For the correlation analysis shown in Fig. 7, we only used those parts of sequences, in which the yaw orientation of wasps was to within ± 10^{o} of the direction parallel to the camera optical axis (marked by grey horizontal bars in Fig. 7A). Note that this is a conservative criterion, because it also discards instances when the insects maintain large pitch angles during roll manoeuvres, which rotates the tip of the abdomen away from the midline.

For the results shown in Fig. 7B and C, we analysed 14 flight episodes, ranging from 0.34 s to 1 s in length (8.14 s of total flight time), from which we extracted 13 sequences that fulfilled this criterion (3.75 s of total flight time), ranging from 0.17 s to 0.43 s in length.

Sequences were stored as .mov-h264 encoded videos and sections showing flying wasps were exported as .jpeg sequences using QuickTimePro (Apple Inc.). The x/y coordinates of the dorsal apex of antennae, the dorsal edge of the head and of the ventral-most point half way between the long dangling hind legs (blue and red dots in Fig. 1E) were extracted frame by frame using a Matlab-based program (Matlab, Nattick, USA), written by Jan Hemmi and Robert Parker (The Australian National University). Head orientation relative to the horizontal and body orientation relative to the vertical (for easier comparison later rotated by 90^{o}) were determined from the x/y coordinates using custom-written Matlab programs. We estimated digitization errors by determining x/y coordinates for one sequence five times (Fig. 7A) and calculating the mean and standard deviations for head and body orientation. The mean standard deviation was in all cases below 2^{o} (see Fig. 7A). The Matlab xcorr function was used to calculate cross-correlations.

Results

We present our chirp data set in Fig. 2 for the four conditions that provided visual input (outdoors, indoors, striped pattern and horizon). Fig. 2 shows over time for each visual condition (see Fig. 1B) the mean value (thick lines) and standard deviation (coloured envelopes) of body orientation ($\theta_{body,}$ blue), head orientation (θ_{head}, red) and the orientation of the head with respect to the body ($\theta_{headbody}$, black mean, green std) for at least two wasps (see Fig. S2 for all individual responses).

We note that head movements never compensate for more than about 50% of the imposed body roll movements at the relatively large oscillation amplitude we used, as is also the case in *Calliphora* (Hengstenberg, 1988). This was true for all conditions, in which pattern contrast was available (outdoors, indoors, stripe pattern and horizon). Perfect head roll compensation would mean that the wasp's head orientation remains constant (i.e., θ_{head} = 0°) and $\theta_{headbody}$ and θ_{body} would change in anti-phase. Compensatory head movement amplitudes were always smaller than the amplitude of the imposed oscillation. In the frequency domain (Fig. 3), this under-compensation is reflected in a negative gain that was always smaller than 0dB (gain < 1) over the frequency range we tested (0.2Hz to 2Hz).

Perfect compensation would mean that the gain between $\theta_{headbody}$ and θ_{body} is equal to 1 (0dB) and the phase is equal to -180° in the Bode plots (as indicated by a black dotted line in Fig. 3B and C). Table 1 shows the mean error between the real head roll compensation of wasps and the perfect case for each experimental condition.

The responses obtained in natural outdoor illumination conditions (Fig. 2 and 3) exhibit smaller gain and phase errors than those obtained for stripe and horizon patterns. Compensation is best in outdoor conditions with a mean gain error of 2dB and a phase error of 9° (N=3, n=5; Table 1). Outdoors, the gain remains nearly constant over the frequency range (blue line in Fig. 3B), but the mean phase value improves in the frequency range from 1Hz to 2Hz, as the frequency of the oscillation increases and the amplitude decreases. We obtained similar results for the gain, but not the phase in the room light condition (red lines in Fig. 3B and C).

The compensatory responses are similar in the striped pattern (green lines in Fig. 3B and C) and horizon conditions (black lines), although gain errors are on average larger than in the outdoor and indoor conditions (Table 1). In all the cases, the maximum mean phase is about -195° corresponding to a mean phase error of 15° (see figure 3C and table 1) which means that the compensatory response has a mean time lag shorter or equal to two sampling periods (40ms, see Fig. 4B). As far as average gain error is concerned, head compensation amplitude is smallest with the artificial horizon, which was the poorest visual stimulus in terms of spatial frequency composition.

To document intra-individual variability, Bode diagrams for three stimulus repetitions outdoors are shown for one wasp in Fig. 3D and E, together with means and standard deviation for an additional individual in the lower panel of Table 1.

When no pattern contrast was available in the uniform bright condition and in complete darkness, there was no evidence of any head roll compensation (Fig. 4A). The weak modulation of head orientation in the uniform condition was most likely caused by some remaining visual structure within the apparatus and the small head movements in the dark condition were in the wrong direction. Head movement amplitudes were too small for the computation of the Bode diagrams. We therefore computed the autocorrelation function of

body orientation θ_{body} and the cross-correlation function between θ_{body} and $-\theta_{headbody}$ (Fig. 4B). Compared to the four conditions that provided visual input, with maximal correlation coefficients between 0.7 and 0.9 and lags between 40 ms and 80 ms, the coefficients do not reach 0.4 in the uniform and -0.4 in the dark condition (Fig. 4B). We conclude that there are no detectable head movements that correlate with the sinusoidal oscillation of the wasps' body.

The responses to imposed step changes in body orientation (Fig. 5) confirm that compensatory head movements are purely visually driven, but also provide two additional pieces of information. Outdoors, the wasps appear to have an absolute reference for head orientation because they were able to maintain a constant compensation angle of up to 20^{o} when the body is turned 45^{o} to the left or to the right (Fig. 5, left column). This cannot be due to a velocity servo, such as the optomotor response of the fly that stabilizes head yaw orientation by minimizing rotational optic flow around the yaw axis. Indeed, in a situation that does not provide angular position information, such as the regular black and white stripe pattern, wasps tend to be unable to keep head orientation constant after a step rotation (centre column, Fig. 5), indicating that the initial response of a velocity servo becomes corrected by a signal that adjusts head position relative to the thorax (Preuss and Hengstenberg, 1992, Gilbert and Bauer, 1998, Paulk and Gilbert, 2006). In full darkness (right column, Fig. 5), the wasp's head orientation in some cases tends to overshoot the imposed rotation of the body and in some cases not. It is not clear at present, why this should be so, but this observation again demonstrates that head orientation is not controlled by haltere-like mechano-sensory input that would help to compensate for body rotations.

We attempted to model step responses of the head roll stabilization system in *Polistes* wasps by considering the angular orientation of the body as an input disturbance for two nested visual feedback loops: an outer speed feedback loop based on the measurement of head orientation (transfer function $H_{Eye}(s)$) and an inner position feedback loop based on the measurement of the head rotational speed provided by wide-field motion sensitive neurons (transfer function $H_{MS}(s)$) with responses that could be similar to those of the VS neurons of the blowfly (Krapp et al. 1998). Fig. 6A shows on the left a block diagram of this

model and on the right the different parameters of the transfer functions used to compute the model responses.

Model responses to 45° step changes of body orientation for $\theta_{head}(t)$ (grey lines in Fig. 6B) and for $\theta_{headbody}(t)$ (red lines, Fig. 6B) are very similar to the step responses we measured outdoors and in the presence of periodic stripes, with the exception of slight differences in steady-state values. Best fits for individual wasp responses required small adjustments in the values of the gain and the time constant of the transfer functions. The $H_{MS}(s)$ cut-off frequency indicates that outdoors, wasps should be able to respond to temporal frequencies of about 8 Hz, compared to 4Hz in the indoor stripe environment.

In free flight, male *Polistes* wasps hold their heads horizontal to within $\pm 10^{o}$ despite body roll movements of more than $\pm 40^{o}$. The four panels of Fig. 7A show the time course of head roll orientation (θ_{head} in red), of body roll orientation (θ_{body} in blue), of the inverse of head orientation relative to the body ($-\theta_{headbody}$ in black) and of the yaw orientation of the longitudinal body axis (in green). The sequence in the top panel of Fig. 7A was digitized 5 times to gain estimates of how accurately head and body orientation can be determined, with thick lines and equivalently shaded areas showing means and plus/minus standard deviation, respectively. Numbers on the right are the mean standard deviations for the four variables. The grey horizontal bars in all panels of Fig. 7A mark the range of $\pm 10^{o}$.

The distributions of head and body roll orientation during 3.75 s of flight (13 sequences, extracted from 14 flight episodes) during which wasps faced away from the camera to within $\pm 10^{o}$ confirm that the wasps keep their head aligned horizontally to within $\pm 10^{o}$ in the presence of body roll movements of up to 40^{o} (Fig. 7B). Body roll oscillations in free flight thus do reach comparable amplitudes to the ones used in our experiments and the quality of head roll stabilization is as good as that reported for honeybees (Boeddeker and Hemmi, 2009). Naturally occurring angular velocities of the body tend to be predominantly below $500^{o}/s$ (Fig. 7B), so that the $245^{o}/s$ we used in our experiments were well within the natural range of velocities. Most surprisingly, in a cross-correlation analysis applied to 13 flight sequences, ranging from 0.17 s to 0.43 s in length, we did not find detectable delays between body roll and head orientation (Fig. 7C, left panel), nor between the angular rates of body and head roll movements (Fig. 7C, right panel). Since our sampling interval was 3.33

ms at 300 fps, it seems unlikely that head stabilization is achieved by visual feedback, unless it is unusually fast in wasps. However, even the fast feed-forward signals from wing-based mechanoreceptors in flies require 3-5 ms to generate a head movement (Sandeman and Markl, 1980; Hengstenberg, 1993).

We did not find evidence for haltere-like mechanosensory input to the head stabilization system in response to imposed body roll rotations. The absence of a detectable and realistic delay in free flight thus suggests that the head may be stabilized by an efference copy signal. We modelled such a feed-forward control of the head orientation (Fig. 7D) as an extension of the two nested visual feedback-loops (Fig. 6A) by considering a common drive signal U_{roll} that elicits a spontaneous roll manoeuvre and controls both head and body orientation around the roll axis. A feed-forward controller $C_f(s)$ makes the head ($\theta_{headbody}$) compensate exactly for any rotation of the body (θ_{body}).

According to the complete block diagram of the proposed head stabilization system (Fig. 7D), assuming that there is no disturbance applied to the body, the orientation of the head can be expressed as:

$$\theta_{head} = G_{body}(s)U_{roll} - G_{head}(s)C_f(s)U_{roll} \quad (4)$$

For perfect compensation of a rotational movement of the body (in our case around the roll axis), the angular orientation $\theta_{headbody}$ must be equal and opposite to θ_{body}, which means that $\theta_{head} = 0$. Then from (4), $C_f(s)$ can be written as:

$$C_f(s) = \frac{\hat{G}_{body}(s)}{\hat{G}_{head}(s)} \quad (5)$$

with $\hat{G}_{body}(s)$ and $\hat{G}_{head}(s)$ the estimated transfer functions of $G_{body}(s)$ and $G_{head}(s)$, respectively. The thick grey and red lines in the three lower panels of Fig. 7A show the output of this model using the following transfer functions:

$$C_f(s) = \frac{0.65}{(1+2.10^{-3}s)} \text{ and } G_{head}(s) = \frac{1}{(1+1.10^{-3}s)},$$

while the other transfer functions remained the same as those used for wasp 1 outdoors (see Fig. 6A). Then from (5), $\hat{G}_{body}(s)$ and $\hat{G}_{head}(s)$ can be written as:

$\hat{G}_{body}(s) = \frac{1}{(1+2.10^{-3}s)}$ and $\hat{G}_{head}(s) = \frac{1}{0.65}$.

In conclusion, the model results are in such close agreement with the free flight behaviour that we suggest a feed-forward control signal to be responsible for the fast compensatory head-roll movements in free flight.

Discussion

We have investigated compensatory head-roll in *Polistes* wasps in tethered flight and found, at least in the frequency range we tested, no evidence for an haltere-like mechano-sensory input that would help to compensate for imposed body roll movements. The extent of the visually driven compensation depends on the light intensity, possibly contrast and on the structure of the visual scene: compensation is best outdoors and becomes weaker under artificial light and visual conditions, such as in a laboratory scene, a 180° black and white pattern or a regular pattern of black and white stripes. Outdoors, wasps are able to maintain a constant, more or less horizontal head orientation after an imposed step rotation, indicating that an outdoor scene provides absolute orientation reference information, such as the overall light distribution or the sun. Wasps are unable to compensate for imposed body roll in uniform bright light and in total darkness. In free flight, wasps keep their head horizontal to within ±10° despite body roll amplitudes of ±40° and angular velocities up to at least 1000°/s.

Admittedly our samples are relatively small and the results of studying control systems in tethered flight need to be interpreted with caution: the tether interferes with the flexible properties of the thorax and in many other respects does not represent free flight conditions. However, within these limits, our results are consistent across animals and stimulus regimes and our free flight analysis suggests that rotation speed and amplitudes were comparable to those occurring most frequently in natural flight. Our data also demonstrate that there are significant differences in how control systems work even in tethered flight, depending on whether they are presented with artificial compared to naturalistic input.

There are a number of reasons why compensatory reflexes in response to imposed body rotations can be expected to perform more reliably under natural conditions. Both photoreceptors (Laughlin and Weckström, 1993; Tatler *et al*., 2000; Juusola and Hardie, 2001a,b) and motion sensitive interneurons (e.g. Egelhaaf *et al*. 2001; Lewen *et al*. 2001) become faster and more reliable as temperature and/or light levels increase. For instance, the response latency and the response reliability of the motion sensitive H1 neuron in blowflies increases significantly with a 8°C increase in temperature (Egelhaaf *et al*., 2001), the response speed and temporal resolving power of fly photoreceptors more than double across the temperature range from 19°C to 34°C (Tatler *et al*., 2000) and the information capacity of fly photoreceptors and ocellar interneurons increases with both light intensity and temperature (Juusola and Hardie, 2001a,b; Simmons, 2011). However, there are many other significant differences between our artificial visual environments and the natural one, such as the distribution of light across the terrestrial and celestial hemispheres, including its spectral composition, its state of polarization and its spatial frequency spectrum. For all these reasons we probably obtained weaker responses under indoor illumination conditions and when wasps were surrounded by a structured environment composed of regular black and white stripe pattern.

These differences are most likely related to the different visual input channels that are known to be involved in the stabilization of the head around the roll axis in insects (for reviews see Hengstenberg, 1993; Taylor and Krapp, 2007). Wasps, like flies and dragonflies, possess ocelli that function as fast horizon sensors (Stange, 1981; Berry *et al*., 2006, 2007), but are also involved, together with the compound eyes in the dorsal light reflex (e.g. Schuppe and Hengstenberg, 1993; Hengstenberg, 1993; Parsons *et al*., 2010). Our successful modelling of step responses required in addition to a velocity servo that minimizes residual image motion across the eye, a position servo that adjusts the absolute orientation of the head. The input to this position servo could either be the overall light distribution such as in the tonic dorsal light response mediated by the compound eyes (cf. Hengstenberg, 1993) or the position of visual features across the visual field that would be most salient in the outdoor condition. It is not clear at this stage, whether the ocelli in wasps could also provide positional information, as they do in dragonflies (Stange, 1981). In our model, we did not consider a phasic component of the dorsal light response, such as it is elicited by the ocelli in

Calliphora (Schuppe and Hengstenberg, 1993; Hengstenberg, 1993). However, for the head roll stabilization, the fast high-pass filtering function of the ocelli could clearly complement the slower low-pass filter of the compound eyes.

Under all experimental conditions, we found the gain of the head roll compensation to be smaller than 1, while in free flight, the wasps were perfectly able to keep their head horizontal at very similar thorax roll amplitudes and angular velocities. We see this as a reminder of two crucial problems with tethered flight experiments: (1) tethered flight interferes severely with the complicated mechanical properties of the thorax flight motor system, including the prosternal organs that may be involved in a mechano-receptive feedback on head position relative to the thorax and (2) it neglects the normal, active state of flight because it prevents feed-forward signals from playing their potentially crucial role in controlling head orientation during spontaneous flight manoeuvres.

In flies, the angular position of the head relative to the body is controlled in closed-loop by means of the prosternal organs (Preuss and Hengstenberg, 1992; Gilbert and Bauer, 1998; Paulk and Gilbert, 2006). For instance, it takes less than 300ms for a flesh fly to compensate for an angular perturbation of 35° applied to the head (Gilbert and Bauer, 1998) and only 30ms for a black soldier fly to pitch its head by 30° (Paulk and Gilbert, 2006). We are not aware that the mechanical and the mechano-sensory coupling between head and thorax have been investigated in *Polistes* wasps. There do not appear to be specific structures such as the prosternal organ, but extensive hair fields across the posterior cuticle of the head that may be in contact with the anterior parts of the thorax (personal observation). We are thus not in the position to explain our observation that during the step response in the dark the head appears initially to be rigidly locked to the thorax and then overshoots in the direction of rotation. If head rotation would be solely governed by inertia in this situation the head would first stay behind and then be pulled in the direction of rotation by some spring or arresting properties of the neck connective. Schilstra and van Hateren (1999a,b) assumed that in the fly *Calliphora* the thorax weighs about 100mg and the head about 10mg. That ratio appears to be only 2 in wasps, because in our model given in figure 7, we obtained a good fit of behavioural performance with body dynamics ($G_b(s)$) 2 times larger than those of the head. It is clearly of interest to determine body dynamics in

hymenopteran insects in more detail in future studies.

Unlike blowflies, which execute fast body roll rotations of up to 2000°/s (Schilstra and van Hateren, 1999a), with a maximum amplitude of ±90° (Hengstenberg, 1988), *Polistes* wasps – as our free flight analysis shows – are sluggish fliers, with long dangling legs extended during flight that lead to slower thorax roll dynamics and therefore requiring head roll compensation of much smaller and slower body rotations (see Fig. 7). Head stabilization outdoors and indoors does become more accurate with increasing frequency up to 2Hz in *Polistes* wasps (see Bode diagrams in Fig. 3B) and in free flight, both wasps and honeybees (Boeddeker and Hemmi, 2010) are able to stabilize their head roll orientation to within ±10° of the horizontal despite body roll oscillations as large as ±45°. Boeddeker and Hemmi (2010) found this to be true in flying honeybees up to maximum roll velocities of 300°/s, which is slightly lower compared to the velocities experienced in natural flight by *Polistes* males (Fig. 7C). We did not detect a noticeable time lag between body roll movements and compensatory head movements in wasps, confirming what Boeddecker and Hemmi (2010) found in freely flying honeybees responding to a rotating pattern. Although such zero-delay responses could theoretically be due to non-linearities and temporal filter properties in the visual pathway, we propose here a vision-based feed-back control scheme enhanced by a feed-forward control of the head orientation (see figure 7). When compensation is effective (see figures 5 and 6), the presence of overshoot in step responses can be explained in our model by a high gain of the visual controller $C_v(s)$.

We note that the time delay we measured in the chirp response analysis can result from a combination of a pure delay that shifts a signal by a fixed amount along the time axis, regardless of its frequency and of phase shifts caused by temporal filters in the signal processing pathways. However, as we did not notice any pure time delay in the step responses, the transfer functions of model responses to 45° step changes (figure 6) do not include any terms accounting for time delays.

The issue of zero-lag responses during spontaneous movements in free flight needs to be addressed in future experiments, possibly using suspended insects that can rotate freely, so that the time lag between compensatory head movements and rotating visual patterns can

be accurately determined. This would also make it possible to identify the cut-off frequency of the visual feedback loops. .

Polistes wasps, like all hymenopteran insects, do not possess modified wings such as the halteres of Diptera and Strepsiptera and wing mechanoreceptors do not appear to provide a fast feed-forward signal of body rotations that could be used to adjust head orientation with a very small latency (about 3 – 5 ms in blowflies, Sandeman and Markl, 1980; Hengstenberg, 1993). Flying wasps never exhibited head compensation in the absence of image motion at imposed body roll frequencies ranging from 0.2Hz to 2Hz and in response to step changes in body roll. As in honeybees (Boeddeker and Hemmi, 2010), gaze stabilization in *Polistes* wasps during enforced thorax roll oscillations thus clearly relies predominantly on visual feedback, involving motion-sensitive interneurons, which by necessity introduces much longer latencies than non-visual, open-loop haltere-derived oculomotor reflexes. In *Polistes* wasps, the largest time delay we found due to phase shift is about 80 ms, comparable to the 30 ms measured in blowflies (Hengstenberg, 1993). An alternative possibility is that our maximal turning velocity of 245°/s was too slow to stimulate potential Coriolis force sensors on the wings. However, halteres in both Diptera and Strepsiptera do respond to rotational velocities as low as 100°/s (Hengstenberg, 1993; Pix *et al*., 1993), so that this is an unlikely reason for why we did not find mechano-sensory input to the head roll control system in *Polistes*.

It remains to be shown, how head roll orientation is controlled in some of the fast flying and hovering Hymenoptera, such as *Bembix* wasps and *Amegilla* bees. *Bembix* wasps, for instance, execute fast saccadic sideways translations by extreme body roll movements of up to 180° amplitude at 2-4000°/s during which the head remains nearly perfectly horizontal (Zeil *et al*., 2008). A possibility is that the motion sensitive neurons in these hovering Hymenoptera are tuned to higher image velocities, as has been shown to be the case in hoverflies and in bumblebees (O'Carroll *et al*., 1996). However, our analysis here suggests that during spontaneous body roll movements, head orientation may be largely controlled by a feed-forward signal, where a copy of the command signals to the wing motoneurons is sent with an opposite sign to the head position servo system (for review see Webb, 2004). In our model, contrary to what has been considered by Varju (1990) and Collett (1980), the

efference copy of the control input signal U_{roll} does not interfere with the inner and the outer visual feedback loops, in the sense that it does not cancel the control input signals $\theta_{headout}$ and $\Omega_{headout}$ to make the head rotate. Our model is also different from the one proposed by Chan et al. (1998), because it does not rely on inhibition of, or a bias introduced in, a sensor (the halteres in this case). Unlike suggested by the reafference (von Holst and Mittelstaedt, 1950), or corollary discharge principle (Sperry, 1950), the output of our forward model ($C_f(s)$) does not serve as input to a sensory processing unit (see Webb, 2004 for review), but controls head orientation in such a way that spontaneous roll body movements do not induce image motion, because the head remains horizontally aligned. In our model, the control signal U_{roll} can be considered as an input reference for controlling the body's orientation around the roll axis. The wasp could benefit from a passive roll stability of its body (see video clips of free flight in supplementary material movies) with a centre of mass placed below the centre of thrust. The feed-forward control proposed here relies only on an accurate internal model of the body's dynamics ($C_f(s)$). In the model shown in figure 7E, the control input signal U_{roll} is copied and sent to the feed-forward controller $C_f(s)$. The latter improves dramatically the performance of the gaze stabilization system during spontaneous rotation of the body because it compensates for the negative phase shift inherent in the two visual feedback loops. Similar feed-forward control has been suggested to explain the high accuracy of vertebrate gaze stabilization during self-generated body movements (Combes *et al*., 2008) and has been successfully implemented in the gaze stabilization system of a sighted aerial robot (Kerhuel *et al*., 2010). We found no delay between head and thorax movements in freely flying *Polistes* wasps and take this as a strong indication that head roll stabilization does involve feed-forward control signals that are inherently difficult to detect and to study in tethered flight. One testable prediction would be that spontaneous changes in wing movements during tethered flight should trigger brief head movements in the opposite direction to the intended body roll rotation.

Acknowledgements

We thank Waltraud Pix for her help with video film analysis, Mark Snowball for advice and Franck Ruffier for fruitful discussions. Marc Boyron assisted in designing and producing the control electronics and the Labview programs. We also thank Julien Diperi for his help with the mechanical construction of the setup.

Funding

This work received support from the Australian Research Council Centre of Excellence program (CE0561903 to JZ) and from the Centre for Visual Sciences at the Australian National University (to SV). SV acknowledges in addition support from the CNRS, Aix-Marseille University, the French National Research Agency (ANR with the EVA project and the IRIS project ANR-12-INSE-0009).

Author contributions

Both authors made equal contributions to conception, design, execution of experiments, to the interpretation of the findings, to the drafting and the revisions of the article.

Table 1

Inter-individual variability	Mean gain error (dB) (N=32)	Mean Std gain error (dB) (N=32)	Mean phase error (degrees) (N=32)	Mean Std phase error (degrees) (N=32)
Outdoors (3 wasps, 5 trials)	8.2	2	9	7.6
Indoors (2 wasps, 2 trials)	10.5	1.9	14.1	1.6
Stripes (3 wasps, 3 trials)	12.3	5.2	5.4	4.6
Horizon (3 wasps, 3 trials)	15.5	4.8	6.2	6.9

Intra-individual variability (3 trials)	Mean gain error (dB) (N=32)	Mean Std gain error (dB) (N=32)	Mean phase error (degrees) (N=32)	Mean Std phase error (degrees) (N=32)
Wasp 1 - Outdoors	7.6	2	4.9	4.8
Wasp 2 - Outdoors	9.2	1.6	15.3	6.2

References

Berry, R., Stange, G., Olberg, R. and van Kleef, J. (2006). The mapping of visual space by identified large second-order neurons in the dragonfly median ocellus. J. Comp. Physiol. A 192, 1105-1123.

Berry, R., van Kleef, J. and Stange, G. (2007). The mapping of visual space by dragonfly lateral ocelli. J. Comp. Physiol. A 193, 495-513.

Boeddeker, N. and Hemmi, J. (2009). Visual gaze control during peering flight manoeuvres in honeybees. Proc. Roy. Soc. B 277, 1209-1217.

Boeddeker, N., Dittmar, L., Stürzl, W. and Egelhaaf, M. (2010). The fine structure of honeybee head and body yaw movements in a homing task. Proc. Roy. Soc. B 277, 1899-1906.Chan, W. P., Prete, F. and Dickinson, M. (1998). Visual input to the efferent control system of a fly's "gyroscope". Science 280, 289-292.

Collett, T. S. (1980). Angular tracking and the optomotor response. An analysis of visual reflex Interaction in a hoverfly. J. Comp. Physiol. 140, 145-158.

Combes, D., Le Ray, D., Lambert, F., Simmers, J. and Straka, H. (2008). An intrinsic feed-forward mechanism for vertebrate gaze stabilization. Curr. Biol. 18, R241-R243.

Dickinson, M.H. (1999). Haltere-mediated equilibrium reflexes of the fruitfly, *Drosophila melanogaster*. Phil. Trans. R. Soc. Lond. B 354, 903–916.

Egelhaaf, M., Grewe, J., Kern, R. and Warzecha, A.K. (2001). Outdoor performance of a motion-sensitive neuron in the blowfly. Vision Res. 27, 3627-3637.

Fox, J.L. and Daniel, T.L. (2008). A neural basis for gyroscopic force measurement in the halters of *Holorusia*. J. Comp. Physiol. A194, 887-897.

Frye, M.A. (2009). Neurobiology: Fly gyro-vision. Curr. Biol. 19, R1119-R1120.

Gilbert, C. and Bauer, E. (1998). Resistance reflex that maintains upright head posture in the flesh fly *Neobellieria bullata* (Sarcophagidae). J. Exp. Biol. 201, 2735–2744.

573 Hengstenberg, R. (1988). Mechanosensory control of compensatory head roll during flight in
574 the blowfly *Calliphora erythrocephala* Meig. J. Comp. Physiol. A 163, 151-165.

575 Hengstenberg, R. (1993). Multisensory control in insect oculomotor systems. In Visual
576 Motion and its Role in the Stabilization of Gaze (ed. F. A. Miles and J. Wallmann), pp. 285–
577 298. Amsterdam, London: Elsevier.

578 Huston, S. J. and Krapp, H. G. (2009) Nonlinear integration of visual and haltere inputs in fly
579 neck motor neurons. *J Neurosci, 29*, 13097-13105

580 Juusola, M. and Hardie, R.C. (2001a). Light adaptation in *Drosophila* photoreceptors: I.
581 Response dynamics and signaling efficiency at 25^{o}C. J. Gen. Physiol. 117, 3-25.

582 Juusola, M. and Hardie, R.C. (2001b). Light adaptation in *Drosophila* photoreceptors: II.
583 Rising temperature increases the bandwidth of reliable signaling. J. Gen. Physiol. 117, 27-
584 41.

585 Kerhuel, L., Viollet, S. and Franceschini, N. (2010) Steering by Gazing: An Efficient Biomimetic
586 Control Strategy for Visually-guided Micro-Air Vehicles. IEEE Trans. on Robotics 26, 307-319.

587 Krapp, H. G., Hengstenberg, B., and Hengstenberg, R. (1998). Dendritic structure and
588 receptive-field organization of optic flow processing interneurons in the fly. J. Neurophysiol,
589 79, 1902-1917.

590 Laughlin, S.B. and Weckström, M. (1993). Fast and slow photoreceptors – a comparative
591 study of the functional diversity of coding and conductances in the diptera. J. Comp. Physiol.
592 A 172, 593–609.

593 Lewen, G. D. and de Ruyter van Steveninck, B. W. (2001) Neural coding of naturalistic
594 motion stimuli. Network 12, 317–329.

595 Ljung, L. (1996), System identification. The control Handbook (W. S. Levine ed.), CRC Press,
596 1033-1054.

597 Ljung, L. (1999). System Identification - Theory for the user. PTR Prentice Hall, Upper Saddle
598 River, New Jersey.

599 Nalbach, G. (1993). The halteres of the blowfly *Calliphora*. I. Kinematics and dynamics. J.
600 Comp. Physiol. A 173, 293–300.

601 Nalbach, G. (1994). Extremely non-orthogonal axes in a sense organ for rotation:
602 behavioural analysis of the dipteran haltere system. Neuroscience 61, 149 –163.

603 Nalbach, G. and Hengstenberg, R. (1994). The halteres of the blowfly *Calliphora*. II. 3-
604 Dimensional organization of compensatory reactions to real and simulated rotations. J.
605 Comp. Physiol. A 175, 695–708.

606 O'Carroll, D.C., Bidwell, N.J., Laughlin, S.B. and Warrant, E.J. (1996). Insect motion detectors
607 matched to visual ecology. Nature 382, 63-66.

608 Parsons, M. M., Krapp, H. G. and Laughlin, S. B., (2010), Sensor fusion in identified visual
609 interneurons. Curr. Biol. 20, 624-628.

610 Paulk, A., and Gilbert, C. (2006) Proprioceptive encoding of head position in the black soldier
611 fly, *Hermetia illucens* (L.) (Stratiomyidae). J. Exp. Biol. 209, 3913-3924.

612 Pix, W., Nalbach, G. and Zeil, J. (1993). Strepsipteran forewings are haltere-like organs of
613 equilibrium. Naturwissenschaften 80, 371-374.

614 Preuss, T. and Hengstenberg, R. (1992). Structure and kinematics of the prosternal organs
615 and their influence on head position in the blowfly *Calliphora erythrocephala* Meig. J. Comp.
616 Physiol. A 171, 483-493.

617 Sandeman, D.C. and Markl, H. (1980). Head movements in flies (*Calliphora*) produced by
618 deflection of the halteres. J. Exp. Biol. 85, 43-60.

619 Sane, S. P., Dieudonné, A., Willis, M. A. and Daniel, T. L. (2007) Antennal mechanosensors
620 mediate flight control in moths. Science 315, 863-866.

621 Schilstra, C., and van Hateren, J.H. (1999a). Blowfly flight and optic flow. I. Thorax kinematics
622 and flight dynamics. J. Exp Biol. 202, 1481-1490.

623 Schilstra, C., and van Hateren, J.H. (1999b). Blowfly flight and optic flow. II. Head
624 movements during flight. J. Exp Biol. 202, 1491-1500.

625 Sherman, A. and Dickinson, M. H. (2003). A comparison of visual and haltere-mediated
626 equilibrium reflexes in the fruit fly *Drosophila melanogaster*. .J Exp Biol. 206, 295-302.

627 Schuppe, H. and Hengstenberg, R. (1993). Optical properties of the ocelli of *Calliphora*
628 *erythrocephala* and their role in the dorsal light response. J. Comp. Physiol. A 173, 143-149.

629 Schwyn, D.A., Heras, F.J.H., Bolliger, G., Parsons, M.M., Krapp, H.G. and Tanaka, R.J. (2011).
630 Interplay between feedback and feedforward control in fly gaze stabilization. Proc. IFAC
631 World Congress, Milano, Italy, 9674-9679.

632 Simmons, P.J. (2011). The effects of temperature on signalling in ocellar neurons of the
633 desert locust, *Schistocerca gregaria*. J. Comp. Physiol. A 197, 1083-1096.

634 Sperry, R.W. (1950). Neural basis of the spontaneous optokinetic response produced by
635 visual inversion. J. Comp. Physiol. Psychol. 43, 482 – 489.

636 Stange, G. (1981). The ocellar component of flight equilibrium control in dragonflies. J.
637 Comp. Physiol. 141, 335-347.

638 Tatler, B., O'Carroll, D.C. and Laughlin, S.B. (2000). Temperature and the temporal resolving
639 power of fly photoreceptors. J. Comp. Physiol. A 186, 399-407.

640 Taylor, G.K. and Krapp, H.G. (2007). Sensory systems and flight stability: What do insects
641 measure and why? Adv. Insect Physiol. 34, 231–316.

642 Varju, D. (1990). A note on the reafference principle. Biol. Cybern. 63, 315-323.

643 von Holst, E. and Mittelstaedt, H. (1950). Das Reafferenzprinzip. Naturwissenschaften 37,
644 464–476.

645 Webb, B. (2004). Neural mechanisms for prediction: do insects have forward models?
646 Trends in Neurosci. 27, 278-282.

647 Xia, X. G. (1997). System identification using chirp signals and time-variant filters in the joint
648 time-frequency domain. IEEE Trans. on Signal Processing 45, 2072-2084.

649 Zeil, J., Boeddeker, N. and Hemmi, J.M. (2008). Vision and the organization of behaviour.
650 Curr. Biol. 18, R320-R323.

651

652 **Figure Legends**

653 Fig. 1 Experimental setup to determine compensatory head roll movements in *Polistes*
654 wasps. (A) Wasps were tethered by waxing a strip of cardboard to their thorax and mounted
655 onto the shaft of a servo motor which was used to rotate the wasps' body. Wasps viewed
656 different visual scenes (B): a natural, outdoor environment (B1), a cluttered and artificially lit
657 indoor laboratory environment (B2), a regular pattern of black and white stripes inside an
658 opaque tube (B3), an artificial horizon (B4), a homogeneous white background (B5), or a
659 completely dark environment (B6). Patterns inside an opaque horizontal cylindrical drum
660 were illuminated with a fibre-optics ring-light and three pairs of infrared LEDs (in case of
661 B6). Wasps were filmed head-on with a digital video camera at 50 or 120fps. (C) Sample
662 images of head and body orientation in the two visual conditions outdoors and with a
663 uniform white pattern. The points on the head and the holding structure that were used to
664 determine orientation are marked by red dots. Note the lack of head roll compensation in
665 the uniform condition. (D) The velocity profile of the chirp signal applied to the servo motor
666 (see Methods for details). (E) Three snapshots from video records of male *Polistes* in free
667 flight. The head and the tip of the abdomen are marked by red and yellow dots,
668 respectively. Their horizontal distance (x), together with independent measurements of the
669 length of the wasps' body long axis (l) was used to estimate the yaw axis orientation (ϕ) of
670 wasps (see schematic on the right). The points used to determine head orientation and body
671 roll orientation are marked with blue dots.

672 Fig. 2 Time course of head roll responses to sinusoidal, frequency modulated (chirp)
673 oscillations applied to the body. In each of the four visual conditions indicated by
674 pictograms (see Fig. 1B for explanation), the mean and standard deviation (coloured
675 envelope) of body orientation (blue), of head orientation (red) and of head orientation
676 relative to the body (black and green) were plotted. The chirp signal frequency increased
677 from 0.2Hz to 2Hz in 20s. Number of wasps and number of chirp runs averaged are given for
678 each panel.

679 Fig. 3 Dynamic properties of the head roll response. (A) The mean chirp responses of the
680 head in the four visual conditions: outdoors, room light, B/W stripes and horizon. (B) Bode
681 diagram for the gain computed from the time-course of responses shown in (A). Thick lines

are means and coloured areas are means ± standard deviation. Dotted line indicates perfect compensation of the head at 0 dB. (C) Bode diagram for the phase (perfect compensation at -180° indicated by dotted line). Otherwise conventions as in (B). Bode diagrams for the gain (D) and phase (E) for three stimulus repetitions outdoors obtained for one wasp.

Fig. 4 Head roll responses in a uniform bright environment and in the dark. (A) Time course of head roll responses to sinusoidal, frequency modulated (chirp) oscillations applied to the body. Conventions as in Fig. 2. (B) Autocorrelation of body oscillations (blue) and cross-correlation of body oscillation against the negative values of head movements relative to the body (red dotted line), for the ideal case: $\theta_{body}(t) = -\theta_{headbody}(t)$. The quality of compensation is indicated by a high correlation coefficient with some delay. Number of wasps and number of responses as in Fig. 2 for conditions horizon, stripes, indoor and outdoor. Uniform: Responses obtained from 3 wasps (N = 3) and 3 chirps in total (n=3). Dark: Responses obtained from 2 wasps (N = 2) and 2 chirps in total (n=2)

Fig. 5 Head roll responses of three wasps (top to bottom row) to step body rotations outdoors (left column), in a cylinder with black and white stripes (centre column) and in the dark (right column). Blue: body orientation; Black: head orientation; Red: head orientation relative to body.

Fig. 6 Modelling head roll stabilization. (A) Left: Block diagram of the head stabilization system in *Polistes* wasps based on two nested visual feedback-loops. Right: Transfer functions of the block diagram described on the left for model responses shown in (B) with s: Laplace variable. The inner feedback-loop receives input on head angular speed (Ω_{head_out}) measured by motion sensitive neurons ($H_{MS}(s)$) while the input to the outer feedback loop is the head orientation (θ_{head_out}) that could be measured by the tonic dorsal light response mediated by the compound eyes. The visual regulator $C_v(s)$ is a simple first order low pass filter removing the high frequency components amplified by the derivative action of $H_{MS}(s)$. The head dynamics are modelled by a first order low pass filter with a time constant of 5ms compatible with the low inertia and mass of the head. (B) Model performance compared to wasp step responses in outdoor and in black and white stripe conditions. Model responses $\theta_{head}(t)$ (thick grey lines) and $\theta_{headbody}(t)$ (thick red lines) were

computed by taking measured body orientation $\theta_{body}(t)$ (blue lines) as input disturbance for the two nested visual feedback-loops. Otherwise conventions as in Fig. 5.

Fig. 7 Head roll control in free flight. (A) Time course of body orientation relative to vertical (blue), head orientation relative to horizontal (red), the inverse of head orientation relative to the body (black) and the yaw orientation of the body longitudinal axis (green) of patrolling *Polistes* males for four example sequences recorded at 300fps. The sequence in the top panel has been digitized 5 times, with means (thick lines) and standard deviations (shaded areas) shown in equivalent colours. Inset numbers are mean standard deviations for the four variables. The horizontal grey areas in all panels mark ±10°. (B) Left: histograms of head orientation relative to horizontal (red) and body orientation relative to vertical (blue); Right: histograms of angular velocity of head (red) and body (blue). Data from 13 sequences, where wasp yaw orientation was within ±10° parallel to the optical axis of the camera; 3.75 s total flight time. (C) Mean cross-correlation functions (black dotted lines) with standard deviation (grey shaded areas) for the same data set as used in (B). Left: head orientation relative to the body ($\theta_{\text{head body}}$) against body orientation (θ_{body}). Right: head angular velocity relative to the body ($\frac{\theta_{\text{head body}}}{dt}$) against body angular velocity ($\frac{\theta_{head}}{dt}$). (D) Expanded block diagram of the proposed head stabilization system in *Polistes* wasps including a feed-forward controller $C_f(s)$ that leads in principle to an exact compensation of head orientation ($\theta_{headbody}$) during spontaneous rotations of the body (θ_{body}). The common drive signal U_{roll} controls both head and body roll orientation, while the two nested visual feedback-loops (see Fig. 6A) provide an absolute orientation reference and correct any remaining slip speed (for details see text). Without any recording of the signal U_{roll}, model responses $\theta_{head}(t)$ (thick grey lines) and $\theta_{headbody}(t)$ (thick red lines) plotted in (A) were computed by taking measured body orientation $\theta_{body}(t)$ (blue lines) as input signal for $C_f(s)$ and as input disturbance for the two nested visual feedback-loops.

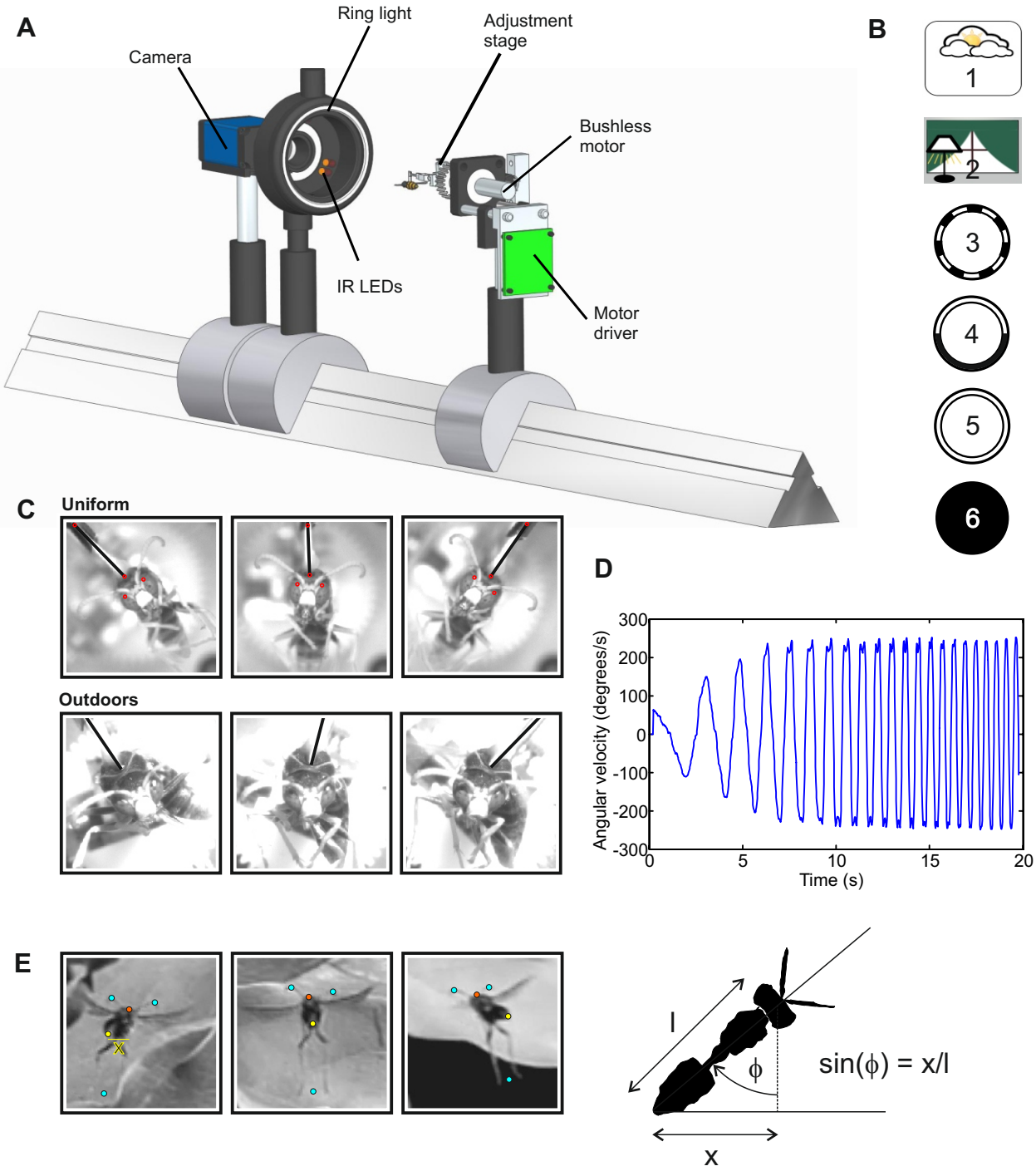

Fig. 1
Viollet & Zeil

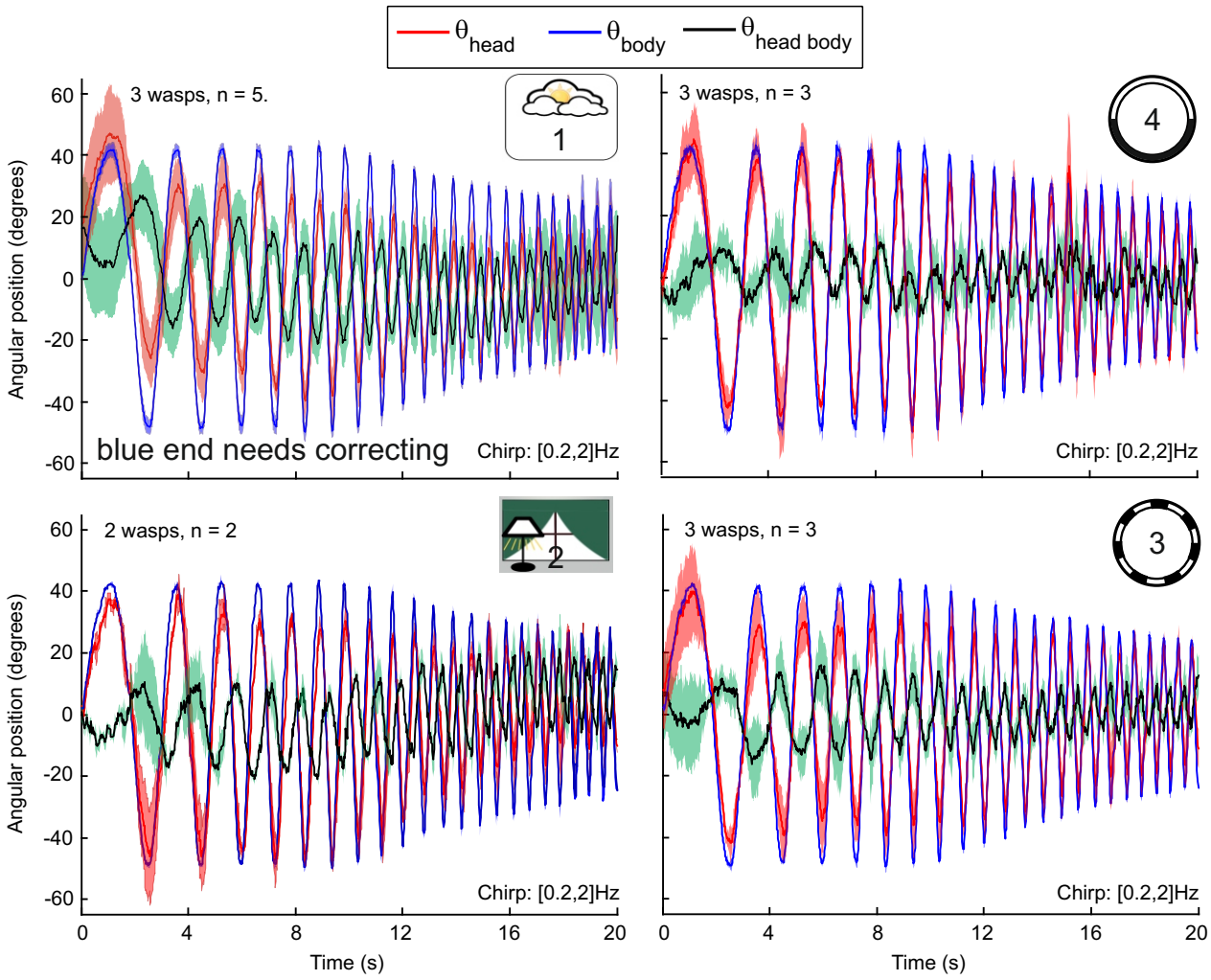

Fig. 2
Viollet & Zeil

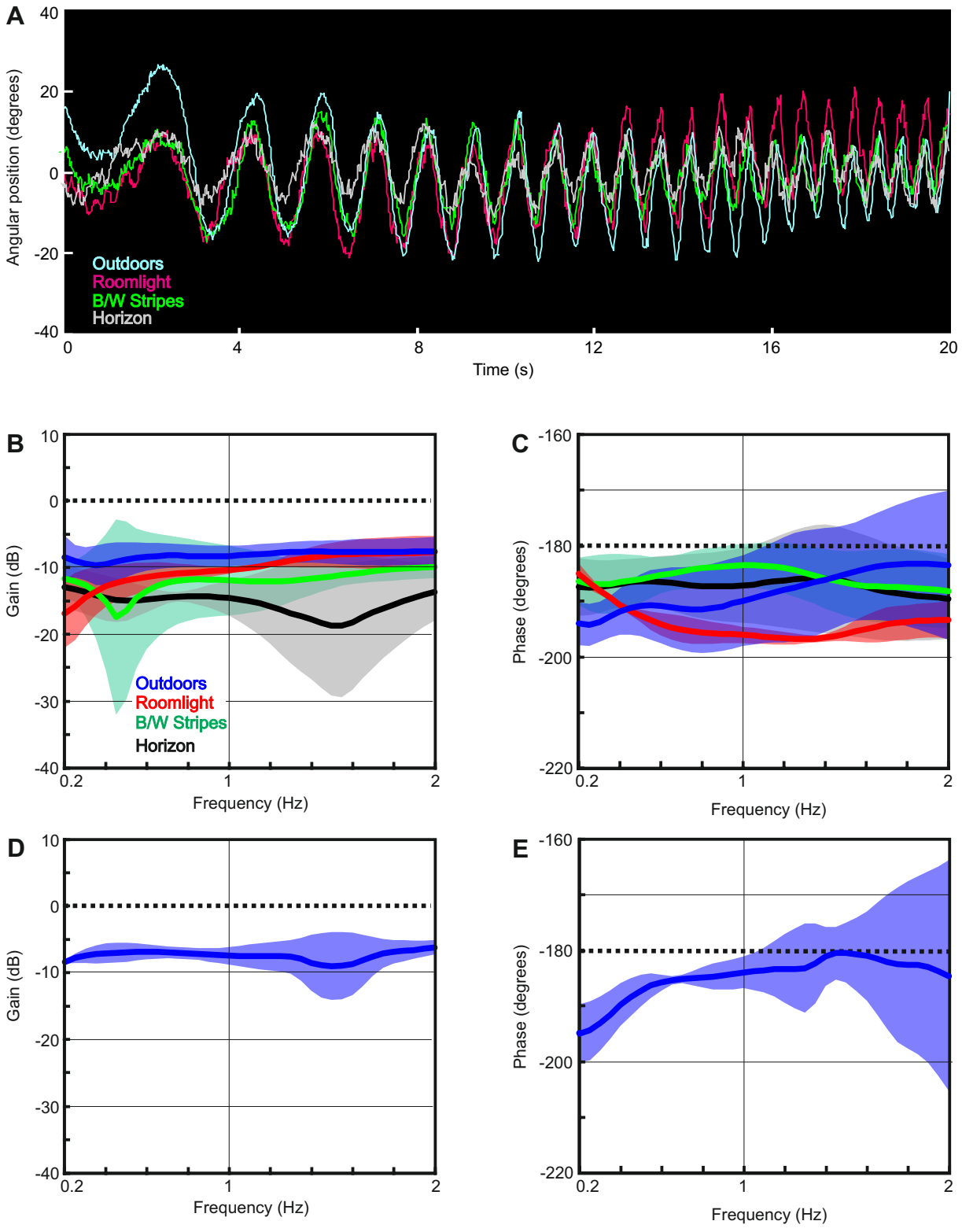

Fig. 3
Viollet & Zeil

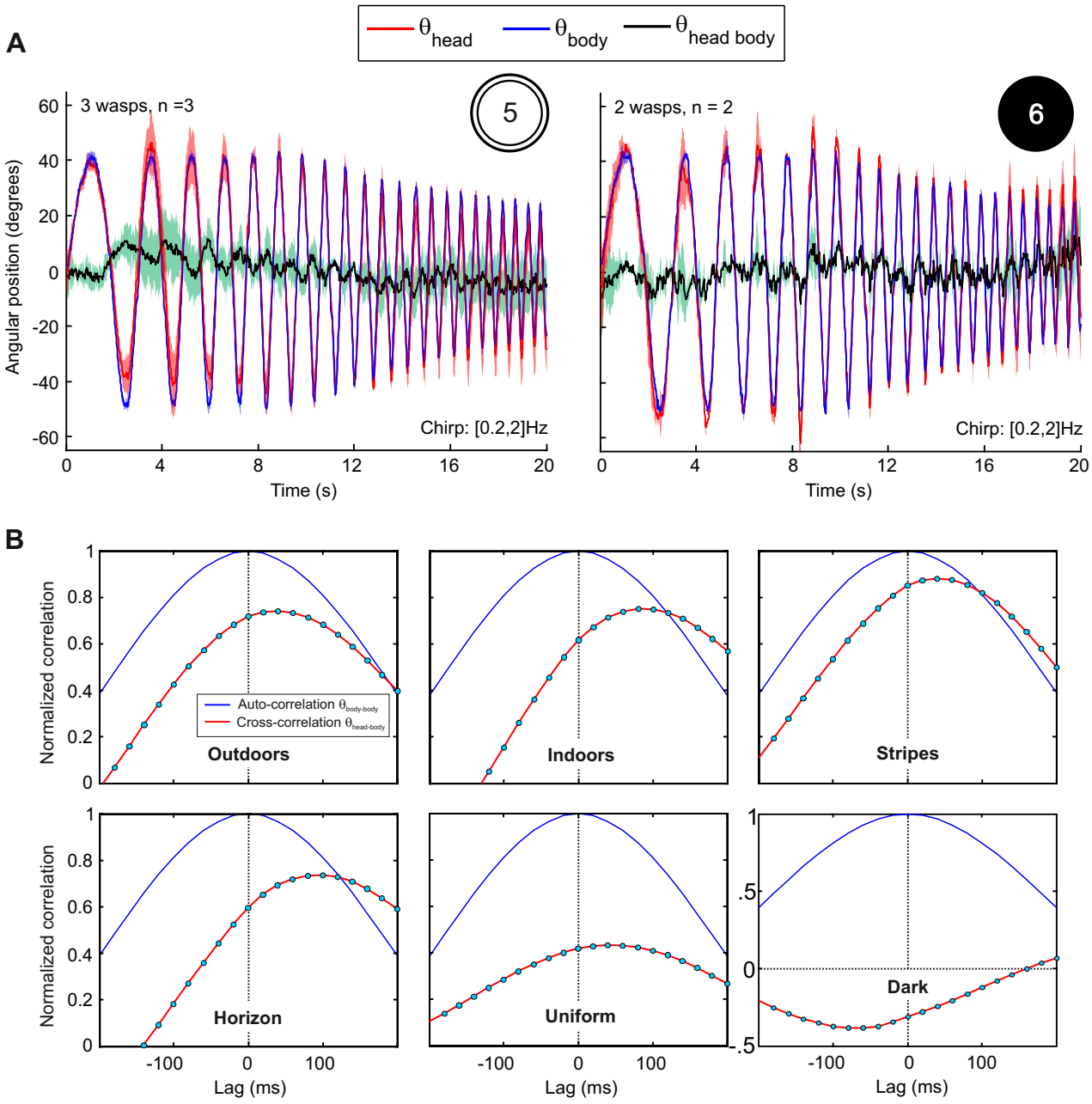

Fig. 4
Viollet & Zeil

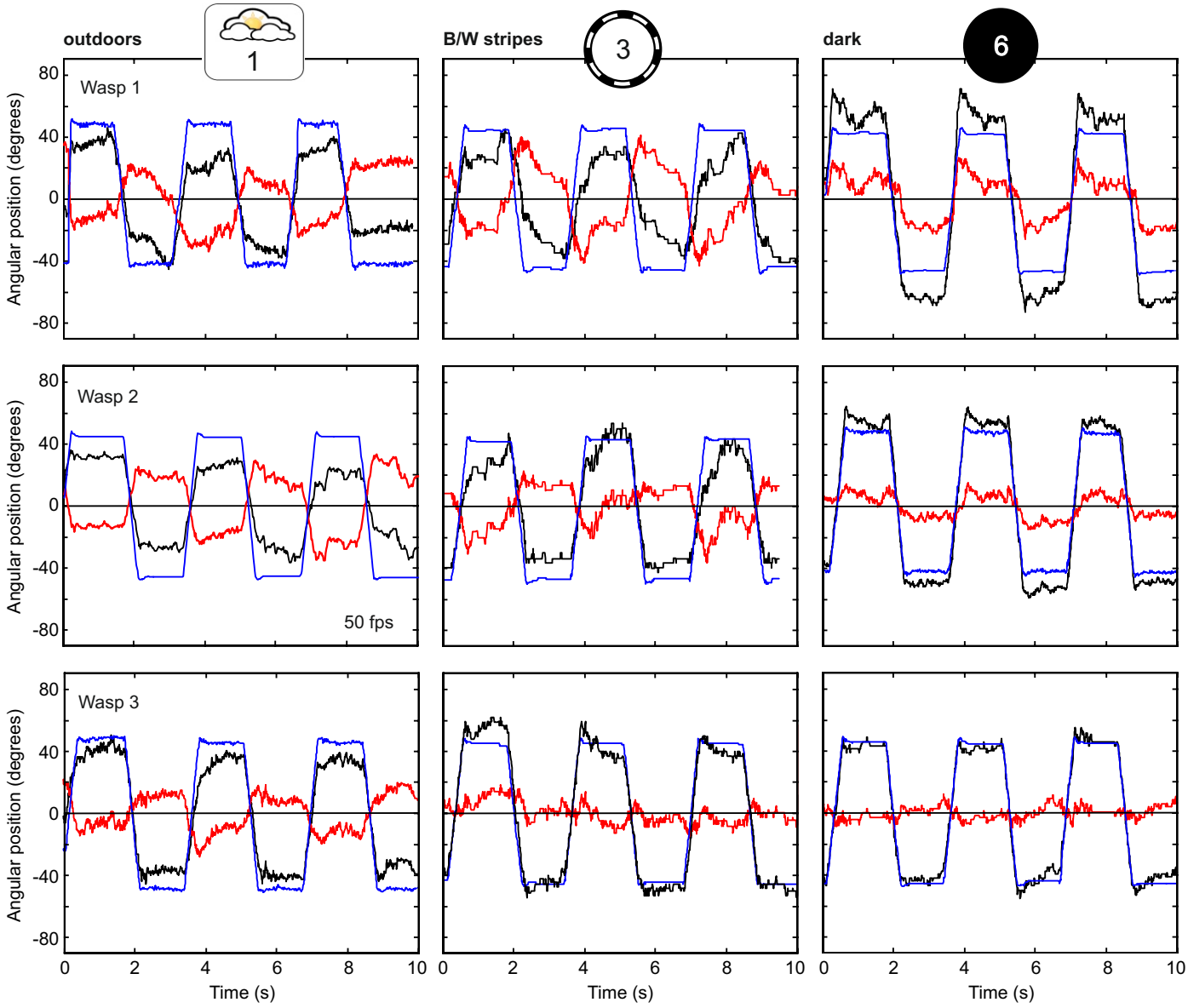

Fig. 5
Viollet & Zeil

A

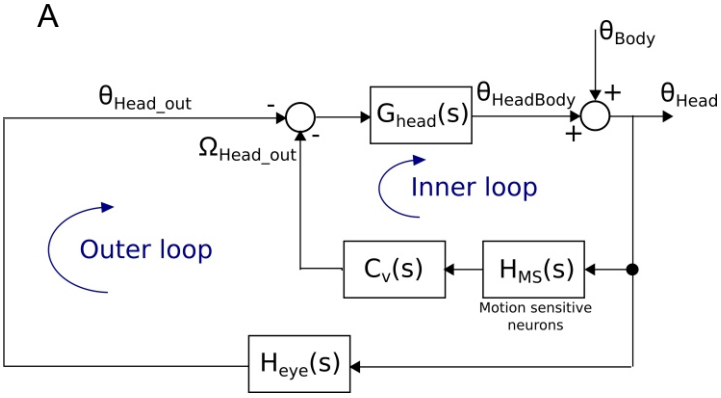

	$H_{MS}(s)$	$H_{eye}(s)$	$C_V(s)$	$G_{head}(s)$
Wasp1 Outdoors	$\frac{0.05s}{(1+0.02s)}$	$\frac{0.25}{(1+0.5s)}$	$\frac{5}{(1+0.5s)}$	$\frac{1}{(1+0.005s)}$
Wasp1 Stripes	$\frac{0.1s}{(1+0.02s)}$	0 (open loop)	$\frac{5}{(1+0.5s)}$	$\frac{1}{(1+0.005s)}$
Wasp2 Outdoors	$\frac{0.05s}{(1+0.02s)}$	$\frac{0.5}{(1+0.5s)}$	$\frac{8}{(1+0.5s)}$	$\frac{1}{(1+0.005s)}$
Wasp3 Outdoors	$\frac{0.04s}{(1+0.02s)}$	$\frac{0.27}{(1+0.5s)}$	$\frac{5}{(1+0.5s)}$	$\frac{1}{(1+0.005s)}$

B

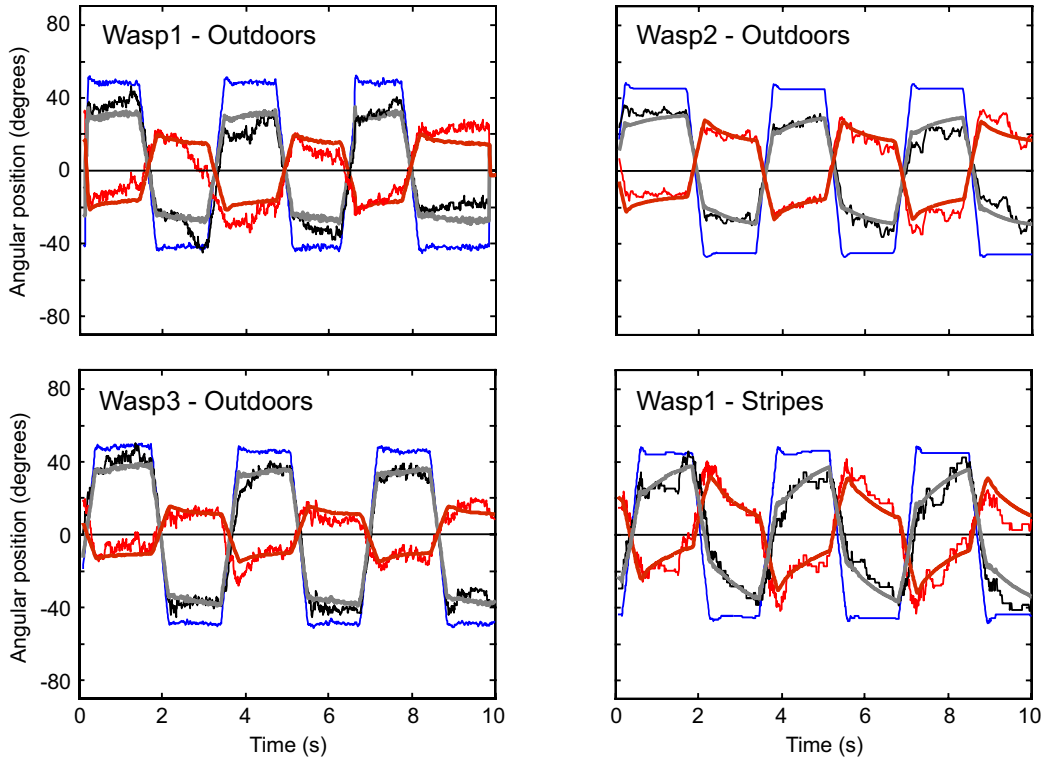

Fig. 6
Viollet & Zeil

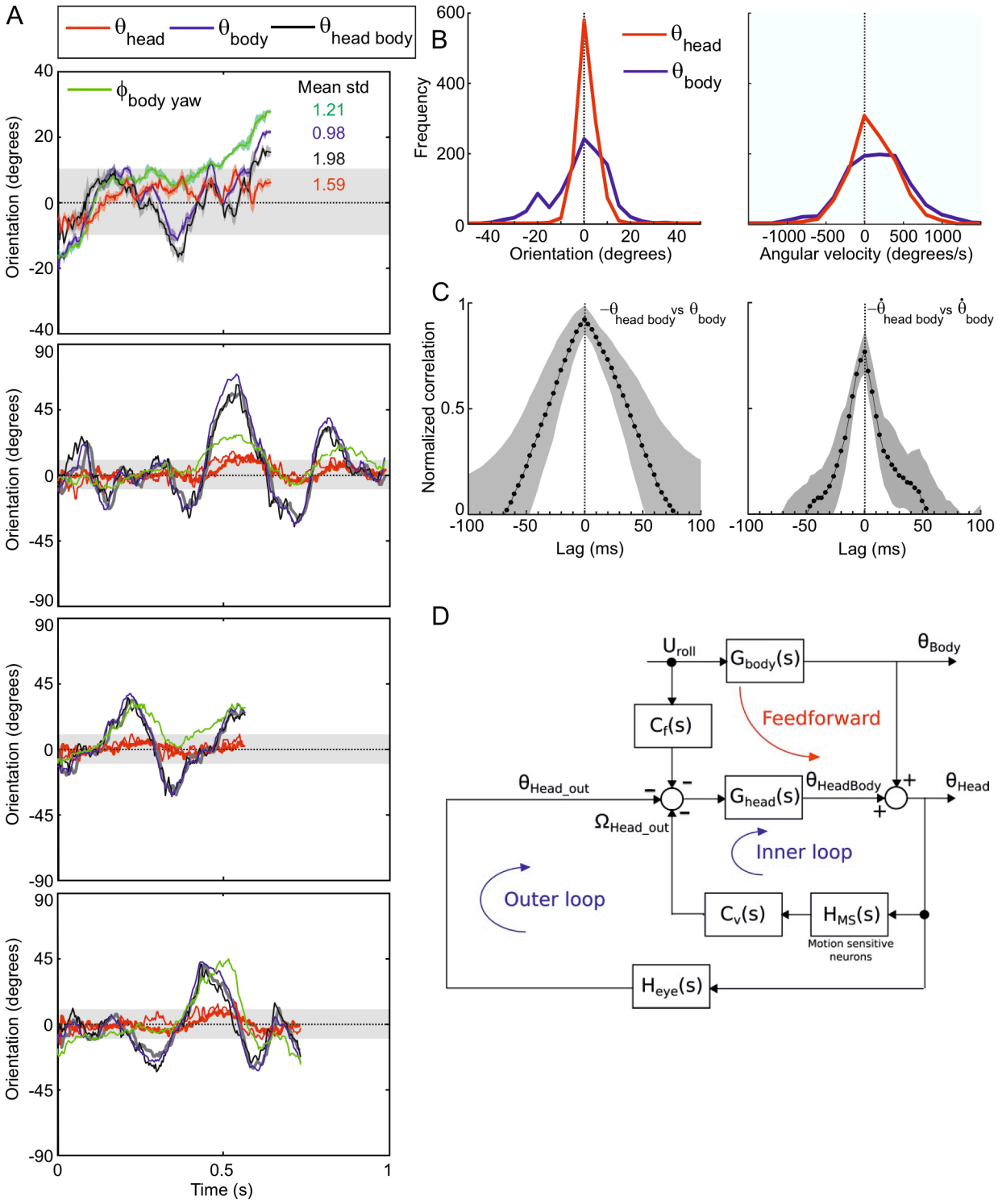

Fig. 7
Viollet & Zeil